Hyperspectral Image Classification by Exploiting the Spectral-Spatial Correlations in the Sparse Coefficients

Dan Liu, Shutao Li, and Leyuan Fang

College of Electrical and Information Engineering,
Hunan University, Changsha, 410012, China
{liudan1,shutao_li,leyuan_fang}@hnu.edu.cn

Abstract. This paper proposes a novel hyperspectral image (HSI) classification method based on sparse model, which incorporates the spectral and spatial information of the sparse coefficient. Firstly, a sparse dictionary is built by using the training samples and the sparse coefficient is obtained through the sparse representation method. Secondly, a probability map for each class is established by summing the sparse coefficients of each class. Thirdly, the mean filtering is applied on each probability map to exploit the spatial information. Finally, we compare the probability map to find the maximum probability for each pixel and then determine the class label of each pixel. Experimental results demonstrate the effectiveness of the proposed method.

Keywords: Hyperspectral image classification, sparse representation, spectral-spatial information, mean filter.

1 Introduction

Hyperspectral image (HSI) is formed by tens to hundreds of continuous and subdivided spectral bands while reflecting interested target areas simultaneously. In HSI, different materials have different spectral information, which can be used for classification.

Many multispectral image classification methods, such as support vector machines (SVMs) [1], [2], neural network [3], and adaptive artificial immune network [4], have been applied to HSI classification. Generally, these methods have obtained good performance.

Researchers show that HSI contains rich spatial information and the pixels in a small neighborhood have similar spectral characteristics. If the pixels are in a small neighbor, they should belong to the same material. Therefore, Some methods [5], [6], [7] have combined spectral information and spatial information, and the classification accuracy has been improved. In particular, the segmentation based method [8] first segment the HSI into many local region with similar spectral characteristics and then classify each region. After using the spatial information, the classifiers can obtain improved performance.

Recently, sparse representation has become a powerful tool to solve some problems, such as face recognition [9], target detection [10], [11], remote sensing image

S. Li et al. (Eds.): CCPR 2014, Part I, CCIS 483, pp. 151–158, 2014.

fusion [12] and medical image reconstruction [13], [14]. Recently, the sparse representation method has also been extended to HSI classification [7], [15], [16]. Basically, the previous sparse representation based HSI classification methods utilize the reconstruction error for the classification. In this paper, we propose a novel method that can combines the spatial information and spectral information in the sparse coefficients for the classification. Firstly, we use the training samples to construct the training dictionary and then utilize the simultaneous orthogonal matching pursuit (SOMP) to obtain the sparse coefficient of each spectral pixel. Differ from other sparse representation based methods which uses the residual to determine the pixel's class, the proposed method first employs the coefficients to construct several probability maps. Subsequently, we exploit the spatial information by filtering every map and gain a probability map for each class. Finally, we can determine the pixel's class by comparing the probability maps.

The rest of this paper is constructed as follows. Section 2 introduces the proposed classification method. Section 3 shows the experimental results and conclusions are given in the section 4.

2 The Proposed Classification Method

Fig. 1 shows the schematic of the proposed classification method. It is constructed by four steps: Firstly, the sparse representation method is adopted to obtain the sparse coefficients. Then, the coefficients belonging to each class are summed to obtain probability map for each pixel. Subsequently, a mean filtering is conducted on each probability map to exploit the spatial information. Finally, classification is accomplished by comparing the maps. The details of each step are illustrated in the follows.

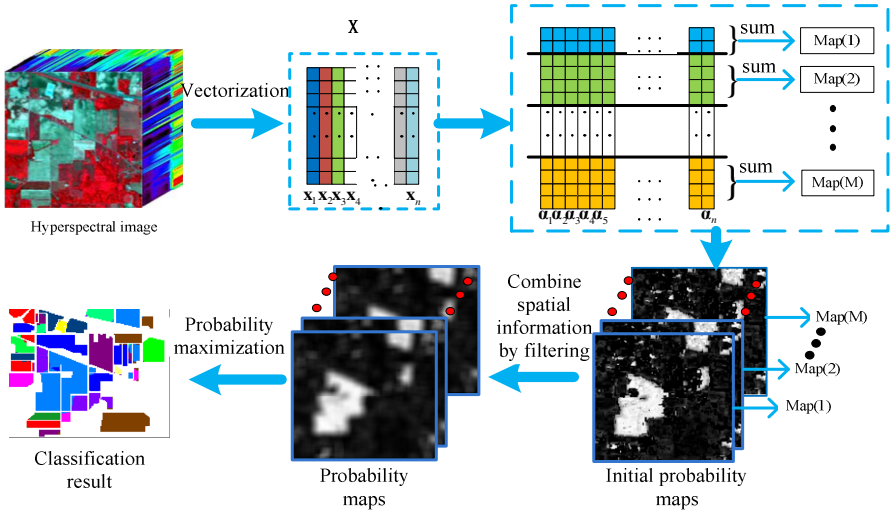

Fig. 1. The scheme of the proposed classification method

Step 1: In HSI, every spectral pixel can be regarded as a vector $\mathbf{x}_i$ and the training pixels construct a matrix $\mathbf{D}=[\mathbf{d_1},\mathbf{d_2},...,\mathbf{d_n}]$ which is called dictionary. Every pixel can be represented by the dictionary.

$$\mathbf{x}_i = \mathbf{d}_1\alpha_i^1 + \mathbf{d}_2\alpha_i^2 + ... + \mathbf{d}_n\alpha_i^n = \mathbf{D}\boldsymbol{\alpha}_i \tag{1}$$

In the equation (1), $\mathbf{d}_1,\mathbf{d}_2,...,\mathbf{d}_n$ is called atom and $\boldsymbol{\alpha}_i=[\alpha_i^1,\alpha_i^2,...,\alpha_i^n]$ is called sparse coefficient vector. The sparse coefficient vector can be obtained by solving the optimization problem.

$$\hat{\boldsymbol{\alpha}}_i = \arg\min \left\|\mathbf{x}_i - \mathbf{A}\boldsymbol{\alpha}_i\right\|_2 \text{ subject to } \left\|\boldsymbol{\alpha}_i\right\|_0 \le K_0 \tag{2}$$

where K_0 is the maximum value of the sparsity level. This optimization problem is a NP-hard and cannot be solved directly. However, it can be solved by greedy algorithms approximately, such as subspace pursuit (SP) [17], orthogonal matching pursuit (OMP) [18] and Simultaneous OMP (SOMP) [7]. In this paper, the SOMP is adopted to obtain the sparse coefficient vector $\hat{\boldsymbol{\alpha}}_\mathbf{i}$ for each spectral pixel $\mathbf{x}_i$.

Step 2: In the sparse coefficient vector $\hat{\boldsymbol{\alpha}}_\mathbf{i}$, there are only a few nonzero sparse coefficients. The larger the nonzero coefficients values in one specific class, the more probability the test pixel belongs to this class. We denote the nonzero coefficients in one class as the $\boldsymbol{\alpha}_{i,m}$, where $m\in\{1,2,...,M\}$, and M is the total number of classes. Then, we sum the nonzero coefficients $\boldsymbol{\alpha}_{i,m}$ for each class of each spectral pixel,

$$\boldsymbol{\alpha}_{i,m}^{sum} = \text{sum}\left(\boldsymbol{\alpha}_{i,m}\right), \quad m\in\{1,2,...,M\}, \text{and } i\in\{1,2,...,N\} \tag{3}$$

where N is the total number of spectral pixels in the HSI. In each class, the summed coefficients $\boldsymbol{\alpha}_{i,m}^{sum}$ for all the spectral pixels in the HSI can construct one probability map z_m.

Step 3: As discussed above, one coefficient in a class probability map z_m can be regarded as the likelihood for the corresponding pixel belonging to this class. If the probability map z_m is directly used for determining the class of each pixel, the spatial information in the probability map is not exploited. To exploit the spatial information, a mean filtering operation is conducted on each z_m,

$$z_m^{meanf} = \text{meanfiltering}\left(z_m\right), \quad m\in\{1,2,...,M\} \tag{4}$$

where the window for mean operation is selected to 3×3.

Step 4: the class label of each pixel $\mathbf{x}_i$ is obtained by comparing the coeffici ents in the filtered probability maps,

$$\hat{m}_i = \max_{m=1,...,M} z_{m,i}^{meanf}(\mathbf{x}_i), \ i\in\{1,2,...,N\} \tag{5}$$

where max is the operation to compute the max coefficient among different maps.

3 Experimental Results

This section tests the effectiveness of the proposed classification method on two real HSIs (Indian pines and Salinas scene). The classification results of the proposed method are compared with those obtained by SVM [19], SVM-CK [20], OMP [7] and SOMP [7]. SVM [19] is designed for the classification of the spectral pixel without utilizing the spatial information. SVM-CK [20] is a method that incorporates spatial information via a composite kernel. OMP and SOMP are two sparse representation based methods.

In our first experiment, we used Airborne Visible/Infrared Imaging Spectrometer (AVIRIS) image Indian pines as testing HSI. This image is a widely used data set and was taken over Indiana's Indian Pine test site in June 1992. The Indian Pines has a size of $145 \times 145 \times 220$, with 220 spectral bands. Because 20 bands is water absorption, these bands are removed. There are 16 ground-truth classes and the size is from 20 to 2455 pixels (the total pixels are 10249).

We chose 10% of the samples for each class as training sample and the remainder as testing samples. For each method, we did five experiments and averaged the results. The number of the training sample and the testing sample is presented in Table 1.In this table, we can see the overall accuracy (OA), average accuracy (AA) and the kappa coefficient by using different methods (the SOMP-P is denoted as our method).

Table 1. Training sets, testing sets and classification accuracy (%) obtained from different methods for the Indian Pines image

Class	Train	Test	SVM	SVM-CK	OMP	SOMP	SOMP-P
Alfalfa	6	40	77.73	91.25	55.12	92.26	**95.04**
Corn-N	144	1284	77.35	92.79	61.60	93.46	**97.77**
Corn-M	84	746	78.56	93.98	58.62	90.22	**97.40**
Corn	24	213	68.75	87.28	42.21	87.32	**95.11**
Grass-M	50	433	88.87	94.90	87.29	**95.20**	94.04
Grass-T	75	655	89.12	**99.51**	95.30	96.12	96.57
Grass-P	3	25	95.37	85.20	85.20	87.10	**87.14**
Hay-W	49	429	95.09	99.91	96.44	99.10	**99.87**
Oats	2	18	67.65	**83.33**	36.67	55.78	0
Soybean-N	97	875	78.64	90.33	71.10	93.45	**93.47**
Soybean-M	247	2208	81.19	96.25	74.11	95.10	**99.20**
Soybean-C	62	531	79.74	89.04	51.05	87.49	**97.61**
Wheat	22	183	92.26	**99.07**	96.85	88.20	97.76
Woods	130	1135	92.72	98.63	91.85	99.00	**100**
Buildings	38	348	69.79	92.64	41.67	83.05	**97.72**
stone	10	83	97.96	90.24	91.90	91.51	**99.35**
OA	-	-	82.91	94.82	73.38	93.66	**97.49**
AA	-	-	83.17	**92.77**	71.06	89.83	91.01
k	-	-	0.805	0.941	0.696	0.931	**0.971**

The Table 1 shows the training sets, testing sets and classification maps obtained by SVM, SVM-CK, OMP, SOMP and SOMP-P and the result is the average of five experiments. From the Table 1, we can see that our algorithm has the best performance in terms of overall accuracy and kappa coefficient. As for its average accuracy, it is only a little worse than the classifier SVM-CK.

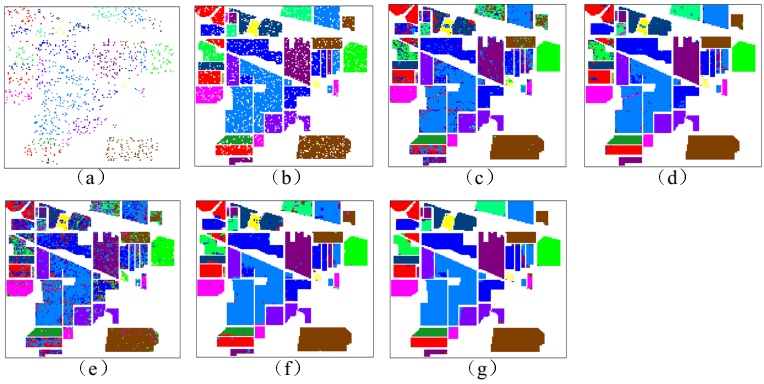

Fig. 2. Indian Pines: (a) Train samples, (b)Test samples, and the classification results obtained by (c) SVM, (d) SVM-CK, (e) OMP, (f) SOMP, (g) SOMP-P

Table 2. Training sets, testing sets and classification accuracy (%)obtained from different methods for the Salinas scene image

Class	Train	Test	SVM	OMP	SOMP	SOMP-P
Weed_1	20	1989	99.88	98.68	**100**	**100**
Weed_2	37	3689	98.52	98.78	99.72	**99.95**
Fallow	20	1956	92.48	94.55	**98.70**	98.41
Fallow plow	14	1380	97.46	99.35	96.93	**99.69**
Fallow smooth	27	2651	97.19	93.26	97.45	**99.24**
Stubble	40	3919	99.98	99.72	99.97	**100**
Celery	36	3543	98.14	99.40	99.55	**100**
Grapes	113	11158	76.11	72.83	84.50	**94.12**
Soil	62	6141	98.63	97.41	99.37	**100**
Corn	33	3245	89.29	88.14	95.24	**98.04**
Lettuce 4wk	11	1057	92.82	96.18	99.26	**100**
Lettuce 5wk	19	1908	96.16	**99.77**	96.73	99.73
Lettuce 6wk	9	907	94.99	98.05	92.53	**99.15**
Lettuce 7wk	11	1059	94.85	90.87	97.40	**99.43**
Vineyard untrained	73	7195	71.90	57.77	**85.24**	83.15
Vineyard trellis	18	1789	98.87	95.06	98.91	**98.92**
OA	-	-	89.16	86.48	93.47	**96.21**
AA	-	-	93.59	92.53	96.13	**98.11**
k	-	-	0.890	0.849	0.9274	**0.958**

In the Fig. 3, (a) and (b) are an example of the training and testing samples. (c) is the classification map obtained from SVM, similarly, (d), (e), (f) are the classification maps of SVM-CK, OMP, SOMP and SOMP-P respectively.

In our second experiment, we use the HSI Salinas scene which was collected by 224-band over Salinas Valley and California. The size of the Salinas image is $512 \times 217 \times 224$. Also, because 20 bands is water absorption which is the same as Indian Pines, the number of bands is reduced to 204. There are 16 ground-truth classes containing vegetables, bare soils, and vineyard fields and the size is from 916 to11271 pixels (the total pixels are 54129).

We chose 1% of the samples for each class as training sample and the rest as testing sample. The number of the training sample and the testing sample is presented in Table 2. In this table, we can see the overall accuracy (OA), average accuracy (AA) and the kappa coefficient by using different methods (the SOMP-P is our method). It is easy to see that the performance of the proposed methods is fine. The Fig. 2 shows the classification maps.

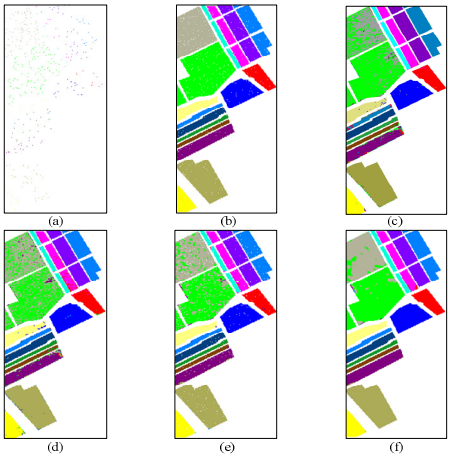

Fig. 3. Salinas scene: (a) Train samples, (b) Test samples, and the classification results obtained by(c) SVM, (d) OMP, (e) SOMP, (f) SOMP-P

4 Conclusions

In this paper, we have proposed a novel HSI classification method base on sparse representation. Differ from other traditional sparse classification technologies which exploit the sparse coefficient and residual to classify directly, this method uses the sparse coefficient to construct probability maps and then exploits the spatial information in the maps for classification. Experimental results show that the proposed method has better performance than several well-known classifiers.

Acknowledgement. This work was supported in part by the National Natural Science Foundation of China under Grant No. 61172161, the National Natural Science Foundation for Distinguished Young scholars of China under Grant No. 61325007.

References

1. Gualtieri, J.A., Cromp, R.F.: Support Vector Machines for Hyperspectral Remote Sensing Classification. In: Proc. SPIE, vol. 3584, pp. 221–232 (1998)
2. Melgani, F., Bruzzone, L.: Classification of Hyperspectral Remote Sensing Image with Support Vector Machines. IEEE. Trans. Geosci. Remote Sens. 42(8), 1778–1790 (2004)
3. Ratle, F., Camps, G.V., Weston, J.: Semisupervised Neural Networks for Efficient Hyperspectral Image Classification. IEEE Trans. Geosci. Remote Sens. 48(5), 2271–2282 (2010)
4. Zhong, Y., Zhang, L.: An Adaptive Artificial Immune Network for Supervised Classification of Multi-/Hyperspectral Remote Sensing Imagery. IEEE Trans. Geosci. Remote Sens. 50(3), 894–909 (2012)
5. Rand, R.S., Keenan, D.M.: Spatially smooth partitioning of hyperspectral imagery using spectral/spatial measures of disparity. IEEE Trans. Geosci. Remote Sens. 41(6), 1479–1490 (2003)
6. Kang, X., Li, S., Fang, L.: Extended Random Walker-Based Classification of Hyperspectral Images. IEEE Trans. Geosci. Remote Sens., 1–10 (May 2014)
7. Chen, Y., Nasrabadi, N.M., Tran, T.D.: Hyperspectral Image Classification Using Dictionary-Based sparse Representation. IEEE Trans. Geosci. Remote Sens. 49(10), 3973–3985 (2011)
8. Driesen, J., Thoonen, G., Scheunders, P.: Spatial Hyperspectral Image Classification by Prior Segmentation. In: IEEE Geosci. Remote Sens. Symp., vol. 3, pp. 709–712 (2009)
9. John, W., Yang, A.Y., Arvind, G., Sastry, S.S., Ma, Y.: Robust Face Recognition via Sparse Representation. IEEE Trans. Pattern Anal. 31(2), 210–227 (2009)
10. Chen, Y., Nasrabadi, N.M., Tran, T.D.: Sparse Representation for Target Detection in Hyperspectral Imagery. IEEE Journal of Selected Topics in Signal Processing 5(3), 629–640 (2011)
11. Fang, L., Li, S., Hu, J.: Multitemporal image change detection with compressed sparse representation. IEEE Image Processing, 2673–2676 (2011)
12. Li, S., Yin, H., Fang, L.: Remote Sensing Image Fusion via Sparse Representations Over Learned Dictionaries. IEEE Trans. Geosci. Remote Sens. 51(9), 4779–4789 (2013)
13. Fang, L., Li, S., Kang, X., Benediktsson, J.A.: Spectral-Spatial Hyperspectral Image Classification via Multiscale Adaptive Sparse Representation. IEEE Trans. Geosci. Remote Sens., 1–12 (2014)
14. Fang, L., Li, S., Ryan, M., Qing, N., Anthony, K.: Fast Acquisition and Reconstruction of Optical Coherence Tomography Image via Sparse Representation. IEEE Trans. Med. Imag. 32(11), 2034–2049 (2013)
15. Fang, L., Li, S., Kang, X., Benediktsson, J.: Spectral-Spatial Hyperspectral Image Classification via Multiscale Adaptive Sparse Representation. IEEE Trans. Geosci. Remote Sens., 1–12 (2014)
16. Fang, L., Li, S., Kang, X.: Spectral-Spatial Hyperspectral Image Classification via Multiscale Adaptive Sparse Representation. IEEE Trans. Geosci. Remote Sens. 52(12), 7738–7749 (2014)
17. Dai, W., Milenkovic, O.: Subspace Pursuit for Compressive Sensing Signal Reconstruction. IEEE Trans. Inf. Theory 55(5), 2230–2249 (2009)

18. Tropp, J., Gilbert, A.: Signal recovery from random measurements via orthogonal matching pursuit. IEEE Trans. Inf. Theory 53(12), 4655–4666 (2007)
19. Gualtieri, J.A., Cromp, R.F.: Support Vector machines for Hyperspectral Remote Sensing Classification. In: Proc. SPIE, vol. 3584, pp. 221–232 (1998)
20. Fauvel, M., Chanussot, J., Benediktsson, J.A.: Adaptive Pixel Neighborhood Definition for the Classification of Hyperspectral Images with Support Vector Machines and Composite Kernel. In: Proc. IEEE Int. Conf. Image Process., pp. 1884–1887 (2008)